# Different Structural and Kinetic Requirements for the Interaction of Ran with the Ran-Binding Domains from RanBP2 and Importin-$\beta$

Carolina I. Villa Braslavsky,[‡,§] Christine Nowak,[‡] Dirk Görlich,[||] Alfred Wittinghofer,[‡] and Jürgen Kuhlmann*[,‡]

*Max-Planck-Institut für molekulare Physiologie, Otto-Hahn-Strasse 11, D-44227 Dortmund, Germany, and Zentrum für Molekulare Biologie, Universität Heidelberg, INF 282, D-69120 Heidelberg, Germany*

*Received May 3, 2000; Revised Manuscript Received July 11, 2000*

ABSTRACT: The cytoplasmic disassembly of Ran·GTP·importin and Ran·GTP·exportin·cargo complexes is an essential step in the corresponding nuclear import and export cycles. It has previously been shown that such disassembly can be mediated by RanBP1 in the presence of RanGAP. The nuclear pore complex protein RanBP2 (Nup358) contains four Ran-binding domains (RanBD*i*) that might function like RanBP1. We used biophysical assays based on fluorescence-labeled probes and on surface plasmon resonance to investigate the dynamic interplay of Ran in its GDP- and GTP-complexed states with RanBD*i*s and with importin-$\beta$. We show that RanBP1 and the four RanBD*i*s from RanBP2 have comparable affinities for Ran·GTP ($10^8-10^9$ $M^{-1}$). Deletion of Ran's C-terminal $^{211}$DEDDDL$^{216}$ sequence weakens the interaction of Ran·GTP with RanBPis approximately 2000-fold, but accelerates the association of Ran·GTP with importin-$\beta$ 10-fold. Importin-$\beta$ binds Ran·GTP with a moderate rate, but attains a high affinity for Ran ($K_D$ = 140 pM) via an extremely low dissociation rate of $10^{-5}$ $s^{-1}$. Association with Ran is accelerated 3-fold in the presence of RanBP1, which presumably prevents steric hindrance caused by the Ran C-terminus. In addition, we show that the RanBD*i*s of RanBP2 are full equivalents of RanBP1 in that they also costimulate RanGAP-catalyzed GTP hydrolysis in Ran and relieve the GTPase block in a Ran·GTP·transportin complex. Our data suggest that the C-terminus of Ran functions like a loose tether in Ran·GTP complexes of importins or exportins that exit the nucleus. This flag is then recognized by the multiple RanBD*i*s at or near the nuclear pore complex, allowing efficient disassembly of these Ran·GTP complexes.

Ran[1] is the major regulator of nucleocytoplasmic transport across the nuclear pore complex [NPC (*1*)]. It is a small Ras-like GTP-binding protein that switches between a GTP- and a GDP-bound form by GTP hydrolysis and nucleotide exchange (*2*−*5*). Ran·GTP is generated from Ran·GDP by nucleotide exchange. This reaction is catalyzed by the exchange factor RCC1 (*6*−*8*). The exclusive nuclear localization of RCC1 (*9*) should ensure that the generation of Ran·GTP is confined to the nucleus. The conversion of Ran·GTP into Ran·GDP is catalyzed by the GTPase activating protein RanGAP1 (*10*−*12*). A fraction of the vertebrate RanGAP1 carries a covalent SUMO1 modification and is tightly bound to the nucleoporin RanBP2 (*13*−*15*). The cytoplasmic localization of free and SUMO-modified RanGAP should ensure that Ran·GTP is depleted from the cytoplasm. This differential localization of the regulators of Ran's nucleotide-bound state should thus result in a Ran·GTP gradient across the NPC which is believed to drive import and export cycles (for recent reviews, see refs *16*−*19*).

Importin-$\beta$-related nuclear transport receptors are thus far the only known regulatory targets of the RanGTPase system. They bind specifically to the GTP-bound form of Ran and use this Ran·GTP binding to regulate cargo loading and unloading. An importin binds its cargo initially in the cytoplasm, is translocated through the NPC, and releases the cargo upon binding Ran·GTP in the nucleus (*20*−*23*). It returns to the cytoplasm as a Ran·GTP complex and without the cargo it just carried in. The removal of Ran·GTP from the importin involves the hydrolysis of the Ran-bound GTP and allows the importin to bind and import the next cargo molecule. Binding of substrates to exportins is regulated in a converse manner as compared to that of importins. Exportins bind their cargoes preferentially in the nucleus, forming a trimeric cargo·exportin·Ran·GTP complex (*24*−*27*). This trimeric complex is then transferred to the cytoplasm where hydrolysis of the Ran-bound GTP results in Ran's irreversible dissociation from the complex, allowing

* To whom correspondence should be adressed: Max-Planck-Institut für molekulare Physiologie, Otto-Hahn-Strasse 11, D-44227 Dortmund, Germany. Telephone: +49 (0) 231-1332104. Fax: +49 (0) 231-1331435. E-mail: juergen.kuhlmann@mpi-dortmund.mpg.de.

‡ Max-Planck-Institut für molekulare Physiologie.

§ Present address: Procter & Gamble, R&D, Sulzbacherstrasse 40, 65823 Schwalbach, Germany.

|| Universität Heidelberg.

[1] Abbreviations: DTE, dithioerythritol; GAP, GTPase activating protein; GST, glutathione *S*-transferase; mantGxP or mGxP, 2′,3′-bis-*O*-(methylanthraniloyl)guanosine di- (D), tri- (T), or 5′-[$\beta$,$\gamma$-imido]-triphosphate (ppNHp), mixture of 2′- and 3′-isomers; mantdGDP or mdGDP, 2′-desoxy-3′-*O*-(methylanthraniloyl)guanosine diphosphate; GppNHp, guanosine 5′-[$\beta$,$\gamma$-imido]triphosphate; Ran, Ras-like nuclear protein product of the human *Ran/TC4* gene; RanΔC, wild-type Ran protein lacking the C-terminal DEDDDL sequence; RanBD*i*, Ran-binding domain *i* of RanBP2; RanBP, Ran-binding protein; RCC1, regulator of chromosome condensation; SDS, sodium dodecyl sulfate; SPR, surface plasmon resonance.

10.1021/bi001010f CCC: $19.00 
Published on Web 08/30/2000

the exportin to release its substrate, re-enter the nucleus, and bind and export the next cargo molecule.

The disassembly of transport receptor·Ran·GTP complexes is thus an essential part of both import and export cycles. However, it is complicated by the fact that these complexes resist GTPase activation by RanGAP (*20*, *28*). RanBP1 can relieve this GAP resistance in all cases tested so far (*27*, *29*−*31*; see also ref *16* and further references therein). RanBP1 has been originally identified as a Ran·GTP binding protein (*32*) and subsequently shown to costimulate RanGAP-dependent GTPase activation in Ran (*12*, *33*). The precise mechanism by which RanBP1 dissociates importin·Ran·GTP and cargo·exportin·Ran·GTP complexes is not fully understood. However, it appears to be clear that the disassembly proceeds through intermediates in which Ran binds simultaneously RanBP1 and the transport receptor (*29*). This ternary complex appears to be in equilibrium with the free transport receptor and a RanBP1·Ran·GTP complex. The latter is an excellent substrate for GTPase activation by RanGAP (*34*) and is removed by GTP hydrolysis from the equilibrium. RanBP1 and RanGAP act catalytically in the disassembly (*29*). Consistent with its function, RanBP1 is excluded from nuclei (*35*) and essential for viability in the yeast *Saccharomyces cerevisiae* (*36*).

The central Ran-binding domain of RanBP1 is called RanBD. Homologous domains have also been detected in a number of other proteins (*37*, *38*). An example is RanBP2 (Nup358) from higher eukaryotes which contains four RanBDs (*39*, *40*). RanBP2 is located at the tip of the cytoplasmic filaments of the NPC. It forms a tight complex with SUMO-modified RanGAP (*13*, *41*). Assuming that the RanBDs from RanBP2 are functional equivalents of RanBP1, then one should also expect the RanBP2·SUMO RanGAP complex to be very efficient in disassembling Ran·GTP transport receptor complexes. However, this still needs to be demonstrated experimentally.

The crystal structure of Ran·GppNHp (GppNHp is a nonhydrolyzable analogue of GTP) in complex with the RanBD1 of RanBP2 has been determined to a resolution of 2.9 Å. The RanBD folds like a PH domain and is involved in extended, intimate contacts with several regions of Ran, in particular with the C-terminal extension of Ran (*42*). This is in contrast to the structure of Ran in complex with Importin-$\beta$ or transportin, where the C-terminal end was either not structured at all (*43*) or only partly visible (*44*).

The structures show that RanBD and importin-$\beta$ bind to essentially nonoverlapping sites on Ran and that the C-terminal end is the major element of Ran discriminating between these two ligands.

Here we show that each of the Ran-binding domains from RanBP2 indeed has properties similar to those of RanBP1. The RanBD from RanBP2 can also stimulate RanGAP-catalyzed GTP hydrolysis on Ran·GTP and form ternary complexes together with Ran·GTP and importin-$\beta$, while ternary complexes between RanBD from RanBP2 (Nup358) have been shown to be formed in vitro (*45*) and on cytoplasmic fibers of the nuclear pore complex (*46*).

We find that the C-terminal end of Ran, while absolutely essential for tight binding to RanBD*i*, is inhibitory with respect to importin-$\beta$ binding. RanBD*i* accelerates the association of importin-$\beta$ with Ran, presumably by sequestering the loose C-terminal extension of Ran.

## MATERIALS AND METHODS

*Chemicals and Enzymes.* All chemicals and enzymes were purchased from Aldrich (Mannheim, Germany), Boehringer (Mannheim, Germany), Fluka (Neu-Ulm, Germany), Merck (Darmstadt, Germany), Serva (Heidelberg, Germany), or Sigma (München, Germany).

*Proteins and Nucleotides.* Ran was expressed in a pET3d vector using *Escherichia coli* BL21DE3 (*47*), and RanBP1 was expressed in a pET11d vector in the same *E. coli* strain. Both proteins were purified as described previously (*48*).

GST fusion proteins of the Ran-binding domains of RanBP2 were cloned in pGEX-2T vectors (Pharmacia) in the group of T. Nishimoto (Kyushu University, Kyushu, Japan). Proteins were expressed from *E. coli* BL21 cells, which were induced with 100 $\mu$M IPTG at an $OD_{600}$ of 0.5 and incubated for 4 h at 37 °C and then overnight at 30 °C. After being harvested, cells were lysed by sonification and purified over a glutathione−Sepharose column.

The importin-$\beta$ fragment of residues 1−462 was expressed from pQE60 with a C-terminal His tag (*49*) in *E. coli* CK600K cells, which were induced at an $OD_{600}$ of 0.6 with 100 $\mu$M IPTG for 5 h at 37 °C. Cells were lysed in 50 mM Tris-HCl (pH 7.5), 20 mM imidazole, 200 mM NaCl, and 1 mM PMSF by sonification; the supernatant was applied over a fast-flow Ni−NTA column (Qiagen) and eluted with an imidazole gradient (50 to 500 mM). After precipitation of importin-$\beta$ with 3 M $(NH_4)_2SO_4$, proteins were dissolved in 50 mM Tris-HCl (pH 7.5).

Proteins were stored in a concentrated form (>2 mg/mL) at −80 °C over a period of 6 months without loss of activity. Loading of Ran with nucleotides was performed as described previously (*7*). Free nucleotide was separated from Ran on a HighTrap gel filtration column (Pharmacia), and the loading efficiency was analyzed by HPLC.

For fluorescence studies, *N*-methylanthraniloyl (mant) derivatives of GDP, GTP, GppNHp, and the corresponding desoxynucleotides were prepared as described by Hiratsuka (*50*) and John et al. (*51*). Concentrations were determined spectroscopically for nucleotides and by using the standard method described by Bradford (*52*) for proteins. All solutions were degassed and filtered before being used.

*Biophysical Experiments.* The basic experimental setup for biophysical analysis with fluorescence-based assays and surface plasmon resonance (SPR) has been described previously (*48*). Fluorescence titration and slow kinetics were analyzed in a SPEX Fluoromax fluorescence spectrometer, and fast kinetics were assessed in an SX16MV stopped-flow system (Applied Photophysics, APP). Because of the instability of Ran in long-term experiments, dissociation reactions of Ran·mGTP·importin-$\beta$ or Ran·mGppNHp·importin-$\beta$ complexes were assessed in 20 mM potassium phosphate buffer (pH 7.4), 5 mM $MgCl_2$, 1 mM $\beta$-mercaptoethanol, and 0.4 g/L BSA. Surface plasmon resonance experiments were carried out in a BIAcore 1000 system (BIAcore). We used a sandwich assay with anti-GST sera (BIAcore) as described previously (*53*) to immobilize GST fusion proteins.

All experiments were performed in HEPES buffer [10 mM HEPES (pH 7.4), 5 mM $MgCl_2$, 0.005% (w/v) Igepal, and 150 mM NaCl] unless indicated otherwise. This buffer was found to be optimal to minimize nonspecific accumulation

in the BIAcore system and to stabilize the anti-GST matrix. Buffers for fluorescence experiments did not contain Igepal.

*Data Analysis.* Stopped-flow experiments were analyzed with the APP software, and slow dissociation experiments were analyzed using GRAFIT 3.0 software and MS EXCEL 97. BIAevaluation 3.0 software (BIAcore) was used for surface plasmon resonance experiments.

*Analysis by Limited Proteolysis.* Proteins and protein complexes were incubated at a concentration of 1 mg/mL in 20 mM $KP_i$ (pH 7.4) and 5 mM $MgCl_2$ with elastase, trypsin, and α-chymotrypsin (all at final concentrations of 4 $\mu$g/mL). Carboxypeptidase A was used at a final concentration of 100 $\mu$g/mL, and the buffer was supplemented with 50 $\mu$M $ZnCl_2$. Incubations were performed at room temperature. Aliquots (10 $\mu$L) were taken at the indicated times points, mixed with 3× SDS buffer, frozen in liquid nitrogen, and subsequently analyzed by SDS−PAGE.

*GTP Hydrolysis Assay.* Ran (40 $\mu$M, preloaded with cold GTP) was incubated with a 10-fold excess of [$\gamma$-$^{32}$P]GTP (diluted with cold GTP to a specific activity of 500 Ci/mol) in 20 mM $KP_i$ (pH 6.5) and 5 mM EDTA for 1 h at room temperature. The reaction was stopped by addition of $MgCl_2$ (final concentration of 10 mM), and free [$\gamma$-$^{32}$P]GTP was removed by gel filtration over a NAP5 column.

Ran·[$\gamma$-$^{32}$P]GTP (1 $\mu$M) was incubated at room temperature in 600 $\mu$L of 64 mM Tris-HCl (pH 7.4), 5 mM $MgCl_2$, and 1 mM DTE in the absence or presence of either 2 $\mu$M RanBP1 or RanBD1 for 10 min. After this preincubation, Rna1 (RanGAP from *Schizosaccharomyces pombe*) was added to a final concentration of 0.15 nM, and 50 $\mu$L samples were taken at various time points, mixed with 350 $\mu$L of charcoal suspension, and centrifuged. Aliquots of the supernatant were counted in a Beckman LS6500 scintillation counter.

## RESULTS

*Conservation of the Ran-Binding Motifs in RanBP1 and RanBP2.* RanBP2 comprises four RanBP1 homologous domains (RanBD*i*, $i = 1-4$; Figure 1A) with an affinity for Ran·GTP high enough to be detected by blot overlay assays (*39*, *40*). The RanBD*i*s contain a highly conserved Ran-binding motif [Figure 1B (*37*, *38*, *54*)]. The fold of RanBD1 (*42*) was shown to be similar to that of the PH domain involved in phosphoinositide binding (*55*), the phosphotyrosine binding domain [PTB (*55*)], and the Ena-Vasp homology domains (*56*) involved in protein−protein interaction. This leads to the notion that this is a domain with a common structure and differing function. The degree of sequence identity between the RanBD*i* and RanBP1 ranges from 45 to 55%. There are similar differences among the RanBD*i*s and between the RanBD*i* and RanBP1. In addition to the conserved RanBD, RanBP1 contains an additional short N-terminus and an approximately 40-amino acid C-terminal extension. The latter has been suggested to contain a nuclear export/cytoplasmic retention sequence (*33*).

Electron micrographs of nuclear pore complexes show cytoplasmic filaments 35−40 nm in length (*57*), which are suggested to be formed among other proteins by RanBP2 (*58*). Blot overlay assays indicated different affinities between Ran·GTP and the individual RanBD*i* of RanBP2 (*40*), leading to speculation about a gradient in affinity from RanBD1 to RanBD4 (*59*). To elucidate such a function, we studied the interaction of Ran with the various RanBD*i*s from RanBP2. These data were compared with the biophysical data for the RanBP1−Ran interaction described previously (*48*).

*Dynamics and Affinities of the Interaction between Ran-Binding Domains of RanBP2 and Ran.* GST fusion proteins with RanBD1 (167 amino acids), RanBD2 (159 amino acids), RanBD3 (155 amino acids), and RanBD4 (150 amino acids) were expressed in *E. coli* BL21 and purified over a GSH−Sepharose column, yielding >95% pure GST fusion proteins. The fusion proteins could be used without thrombin cleavage because the GST moiety was found to have only a negligible influence on the interaction of RanBP1 with Ran (*48*). Two approaches were used to quantify the dynamic parameters of the RanBD*i*−Ran interaction.

Fluorescence assays make use of the increase in fluorescence upon binding of RanBD*i* to Ran complexed with the fluorescently labeled, noncleavable GTP analogue mGppNHp. Saturation of Ran·mGppNHp with RanBD*i* results in an approximately 1.5-fold increase in fluorescence yield, which is linear with the concentration of the Ran−RanBD*i* complex.

Association kinetics were studied by stopped-flow experiments with an SX17MV system (Applied Photophysics), recording the fluorescence increase after mixing different concentrations of RanBD*i* with a constant amount of Ran·mGppNHp. Single-exponential analysis yielded apparent rate constants for pseudo-first-order reactions, which were plotted as a function of the amount of free RanBD*i* to provide the $k_{on}$ for the second-order reaction (Figure 2).

To measure the dissociation rates of the Ran·mGppNHp·RanBD1 complex, an excess of nonfluorescent Ran·GppNHp was added to trap transiently released RanBD1. The concentration of the Ran·mGppNHp·RanBD1 complex was followed over time using the fluorescence assay described for the association kinetics. However, in this case, the dissociation reactions were sufficiently slow to be measured in a standard fluorescence spectrometer.

In a second approach, binding and dissociation kinetics between Ran and RanBD*i* were assessed by surface plasmon resonance with a BIAcore instrument (*60*−*62*). We used a sandwich assay with anti-GST sera covalently bound to the dextran matrix of the sensor surface as described for RanBP1 (*48*). The association and dissociation rate constants for the four individual Ran-binding domains were calculated and compared to the fluorescence data. The reactions were assessed at physiological ionic strength. Table 1 summarizes the kinetic data obtained and compares them with data obtained for GST·RanBP1.

Binding of Ran·GTP to each of the four RanBD*i*s from RanBP2 occurs at $k_{on}$ rates in the range of $10^5$ $M^{-1}$ $s^{-1}$, while dissociation rate constants vary between $10^{-3}$ and $10^{-4}$ $s^{-1}$. Deletion of the C-terminal DEDDDL sequence of Ran reduces the association rate constant by a factor of 100 ($k_{on} = 1.8 \times 10^3$ $M^{-1}$ $s^{-1}$ for RanBD1).

$K_D$, $k_{on}$, and $k_{diss}$ values derived from SPR and fluorescence-based measurements are in good agreement with each other. For the association rate constants, BIAcore and stopped-flow kinetic data were analyzed on the basis of Ran·(m)GppNHp or GST·RanBD*i* concentrations, respectively (pseudo-first-order kinetics). This leads to an additional independence of

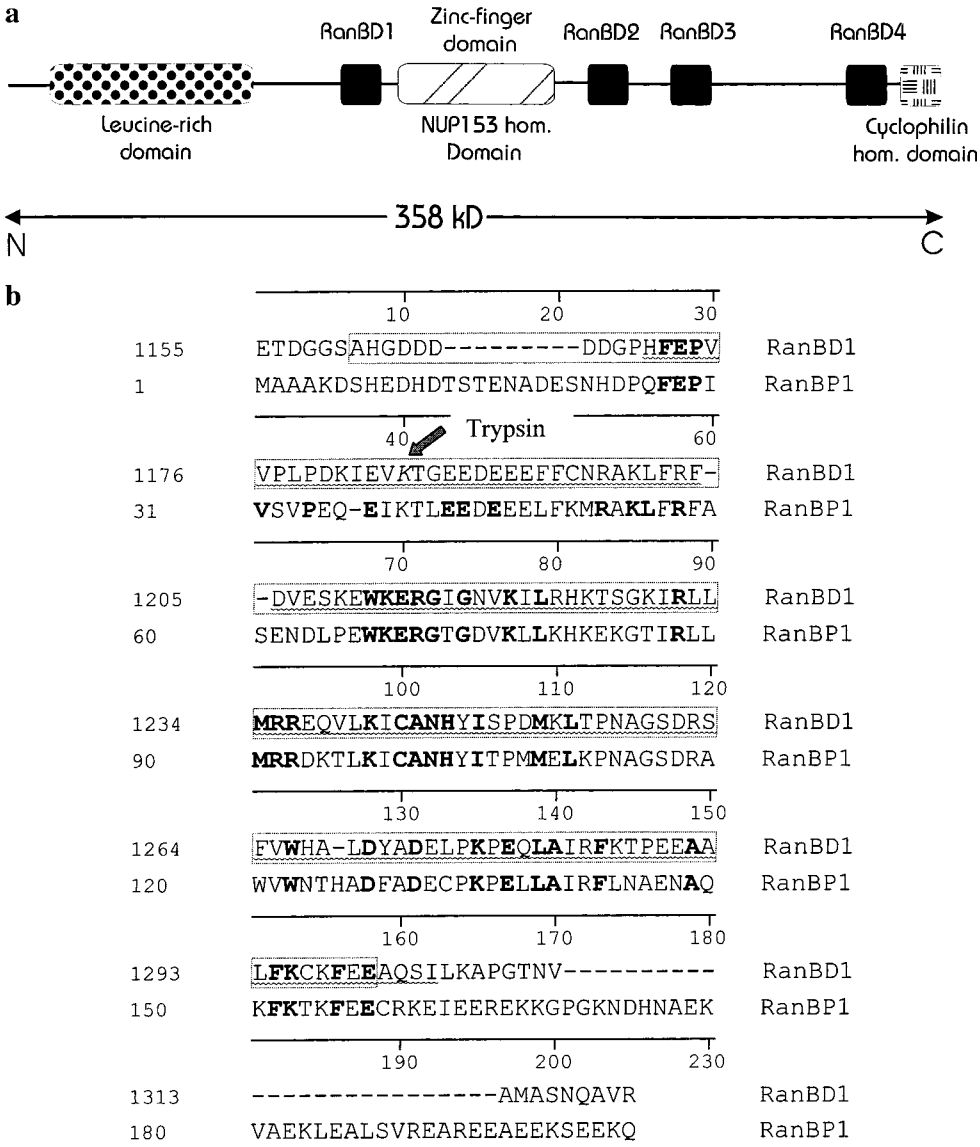


FIGURE 1: (a) Schematic structure of RanBP2. RanBD is the Ran-binding domain. (b) Alignment of RanBP1 and RanBD1 of RanBP2. The amino acid sequences of RanBP1 (AC X83617) and RanBP2 (AC D42063) were aligned by the GCG program. Dashed lines represent gaps inserted to achieve a maximum level of homology. Residues conserved in all RanBD*i*s of RanBP2 and RanBP1 are indicated by bold letters. The box marks the minimal Ran-binding domain; the corrugated line represents residues of RanBD1 defined in the structure of the Ran·RanBD1 complex. The arrow shows the trypsin cleavage site in RanBD1 in the absence of Ran·GppNHp.

the corresponding data sets, because errors in the determination of the active concentration for one of the proteins in, e.g., the stopped-flow experiments, are not propagated in the SPR measurements.

Ran·(m)GppNHp binds the RanBD*i* from RanBP2 with a similar or slightly weaker affinity than the full-length RanBP1 (Tables 1 and 2). The Ran-binding domain alone is sufficient for high-affinity binding of Ran in the GTP state with $K_D$ values in the nanomolar range. The data also show that the rate (Table 1) and equilibrium constants (Table 2) of the individual RanBD*i*s of RanBP2 are comparable to each other. There exists no gradient in affinity, which would support the idea of a guided walk of Ran along the RanBP2 protein.

*The N-Terminal Sequence of the Ran-Binding Domains Is Essential for Recognition of Ran.* On the basis of sequence similarity, a minimal RanBD has been defined as an approximately 150-residue fragment that can be stably expressed in *E. coli* and that is able to bind to Ran (*54*). The structure of RanBD1 in complex with Ran·GppNHp has shown that the N-terminal part of this domain is not part of the PH domain-like fold, but is an extended chain that reaches over to Ran and is involved in a number of contacts (*42*).

The first 16 acidic amino acids of the RanBD1 N-terminus were not visible in the electron density of the complex. To probe the structure of RanBD in this area, we performed a limited proteolysis of RanBD1 with trypsin. It produced a stable fragment lacking the N-terminal 31 amino acids of RanBD1 as judged by SDS−PAGE (Figure 3a) and mass spectroscopic analysis. The presence of stoichiometric amounts of Ran·GppNHp protected the N-terminus of RanBD1 from trypsin cleavage (Figure 3b), suggesting also that the N-terminal highly acidic residues are involved in contacts with Ran. Indeed, the truncation of these first 31 amino acids in RanBD1 diminished the affinity for Ran·GppNHp dramatically. Since no complex formation could be observed by our techniques, $K_D$ values are estimated to be $>50$ $\mu$M (data not shown).

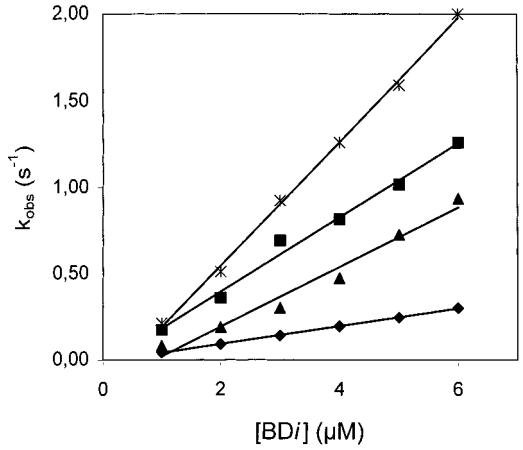


FIGURE 2: Association of Ran·mGppNHp with Ran-binding domains of RanBP2. Stopped-flow kinetics after mixing of 200 nM Ran·mGppNHp with varying concentrations of different GST-RanBP2$^{RanBDi}$ were measured in an APP SX17MV instrument. Data were fitted with a single-exponential equation to yield $k_{obs}$ for the pseudo-first-order reaction. A plot of $k_{obs}$ vs [GST-RanBD*i*] results in a linear trace with a slope $k_{on}$ for the individual RanBD*i*: (◆) RanBD1, (■) RanBD2, (▲) RanBD3, and (*) RanBD4.

Table 1: Kinetic Parameters for Ran·(m)GppNHp Interaction with GST·RanBD*i* from RanBP2[a]

| | $k_{diss}$ ($\times 10^4$ $s^{-1}$) | | $k_{on}$ ($\times 10^{-4}$ $M^{-1}$ $s^{-1}$) | |
|---|---|---|---|---|
| domain | SPR | fluorescence | SPR | fluorescence |
| RanBD1 | 2.5 | 4.2 | 5.8 ± 1.6 | 5.5 |
| RanBD2 | 4.8 | 8.4 | 23 ± 11 | 21.5 |
| RanBD3 | 11 | 14 | 5.3 | 17 |
| RanBD4 | 17 | 4.7 | 9.2 | 35 |
| RanBP1 | 3.7 | 10.5 | 30 | 30 |

[a] Dissociation experiments were performed as duplicates, and only selected domains were analyzed in repeated association reactions.

Table 2: Affinities of Ran·GppNHp for GST·Ran-Binding Domains of RanBP2 in Nanometers

| | BIAcore | fluorescence | | BIAcore | fluorescence |
|---|---|---|---|---|---|
| RanBD1 | 4.3 | 7.5 | RanBD4 | 1.8 | 1.3 |
| RanBD2 | 2.1 | 3.9 | RanBP1 | 1.2 | 3.5 |
| RanBD3 | 20.8 | 8.2 | | | |

*Dynamic Aspects of the Ran−Importin-$\beta$ Interaction.* Affinities of Ran for importin-$\beta$ have so far been estimated only by competition of EDTA- or RCC1-stimulated nucleotide exchange in Ran·GTP or by inhibition of the RanGAP-mediated GTPase reaction of Ran to be in the order of 0.3 nM (*20*). To determine the equilibrium constant in a direct approach and to study the dynamic behavior of the Ran−importin-$\beta$ interaction and its requirements, we verified that formation of a binary complex with importin-$\beta$ causes an increase in the fluorescence intensity of the mant group in Ran·mGppNHp. Hence, it should be possible to assess association and dissociation reactions in the same manner as described previously for the RanBD*i* and RanBP1. We studied an importin-$\beta$ fragment comprising residues 1−462 which has previously been shown to be sufficient for tight binding (*49*), a finding that has been verified by the crystal structure of the complex of this fragment with Ran·GppNHp (*43*).

In stopped-flow kinetics, importin-$\beta$ exhibits slow association with Ran·mGppNHp. Figure 4 shows the fluorescence increase upon binding of 200 nM Ran·mGppNHp to either 6 $\mu$M GST·RanBD2 or 6 $\mu$M importin-$\beta$ (residues 1−462) using the same buffer conditions and temperature. While the half-time of the reaction is about 0.4 s in the case of the RanBD*i*, it takes approximately 8 s for the fluorescence signal to reach its half-maximum change for importin-$\beta$ (Figure 4). The resulting association rate constant is thus 20-fold smaller than the corresponding value for RanBP1.

While no difference could be found in the association rate constants of Ran·GTP and Ran·GppNHp with RanBP1 and the Ran-binding domains of RanBP2 (data not shown), importin-$\beta$ discriminates strongly between Ran·GTP and

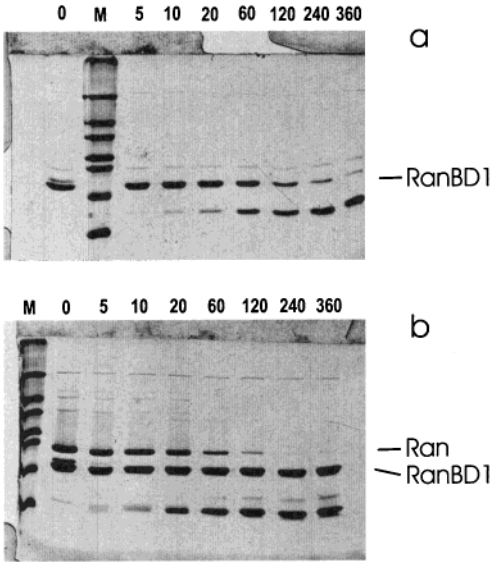


FIGURE 3: Proteolytic digestion of RanBD1 with trypsin. (a) RanBD1 (100 $\mu$g) of RanBP2 was incubated with 0.4 mg/L trypsin in a total volume of 200 $\mu$L at room temperature. Proteolysis products were analyzed by SDS−PAGE after the indicated digestion times (in minutes). Mass spectroscopic analysis of the stable reaction product resulted in a molecular mass of 15 657 Da, indicating cleavage after K31. (b) Same as panel A but with 200 $\mu$g of a Ran·GppNHp·RanBD1 complex incubated with trypsin. While the Ran band is degraded, RanBD*i* runs at the same position even after treatment with protease for 6 h.

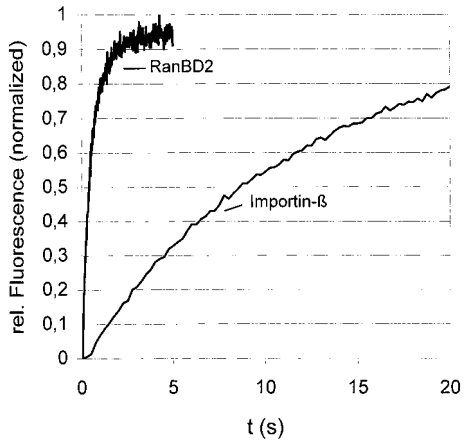


FIGURE 4: Association of Ran·mGppNHp with importin-$\beta$ or RanBD*i*. Ran·mGppNHp (200 nM) was mixed with either 6 $\mu$M importin-$\beta$ (residues 1−462) or GST·RanBP2$^{RanBD2}$ in an APP SX17MV stopped-flow instrument. While the increase in the magnitude of the fluorescence signal is completed for the RanBD2 within <0.5 s, the reaction with importin-$\beta$ is more than 1 order of magnitude slower under the same conditions (20 °C, HEPES buffer). Traces were normalized concerning their amplitude.

Table 3: Association Rate Constants $k_{on}$ ($M^{-1}$ $s^{-1}$) of the Interaction between Importin-$\beta$ (residues 1−462) and Ran as a Function of the Nucleotide and Ran C-Terminus

| | GTP | GppNHp | mGTP | mGppNHp | mGDP |
|---|---|---|---|---|---|
| fluorescence | | | | | |
| Ran | | | $8.5 \times 10^4$ | $1.3 \times 10^4$ | |
| RanΔC | | | | $14.3 \times 10^4$ | $1.2 \times 10^3$ |
| RanC4A | | | | $11.9 \times 10^4$ | |
| surface plasmon resonance | | | | | |
| GST-Ran | $1.0 \times 10^4$ | $0.2 \times 10^4$ | | | |

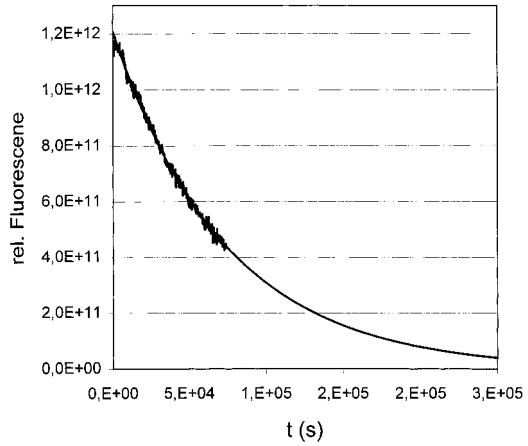


FIGURE 5: Dissociation of the the Ran·mGTP·importin-$\beta$ complex. Ran·mGTP (400 nM) was mixed with 800 nM importin-$\beta$ (residues 1−462) in $KP_i$ buffer [20 mM $KP_i$ (pH 7.4), 5 mM $MgCl_2$, 1 mM DTE, and 0.1 g/L BSA] at 20 °C and mant fluorescence observed in a Fluoromax-2 fluorescence spectrometer (SPEX). Five minutes after mixing was carried out, an excess of 4 $\mu$M Ran·GppNHp was added and the change in the signal was recorded. While a slow decrease in the signal could be observed in the competition experiment, the control without Ran•GppNHp showed a slow increase in the signal. Subtraction of the control signal from the competition experiment was used for the calculation of the net kinetic. Data were fitted as single exponentials.

Ran·GppNHp. In both experimental setups, fluorescence and SPR, $k_{on}$ is about 6 times higher if Ran is complexed with GTP (Table 3).

To analyze the dissociation of the Ran·GppNHp·importin-$\beta$ complex, an excess of Ran·GppNHp was added to compete with rebinding of importin-$\beta$ to the fluorescent Ran·mGppNHp. The spontaneous dissociation of the Ran·importin-$\beta$ complex is, however, very slow, and measuring times of ~20 h were thus required to obtain reaction amplitudes that were high enough for kinetic analysis. Due to the instability of Ran at temperatures of >20 °C or in long-time experiments with an excess of competing Ran·GppNHp, a strong tendency of aggregation was observed. This aggregation could be largely prevented by using phosphate buffer supplemented with 0.4 g/L BSA.

Figure 5 shows the dissociation of a Ran·mGTP·importin-$\beta$ complex corrected for a slow increase in the fluorescence signal in the absence of competitor. Here, no significant differences in the dissociation reaction could be observed for Ran·mGppNHp and Ran·mGTP (Table 4). From this, we can calculate an equilibrium dissociation constant for the Ran·mGppNHp·importin-$\beta$ complex of 1 nM and for the Ran·mGTP·importin-$\beta$ complex of 140 pM.

In our SPR-system, dissociation reactions with such extremely low $k_{diss}$ values cannot be assessed, because the slow release of the antibody·GST complex will mask the dissociation reaction of GST·Ran and importin-$\beta$.

Table 4: Dissociation of Ran·Importin-$\beta$ (residues 1−462) Complexes

| | $k_{diss}$ (s) |
|---|---|
| Ran·mGTP | $(11.6 \pm 1.7) \times 10^{-6}$ |
| Ran·mGppNHp | $9.0 \times 10^{-6}$ |
| **RanΔC·mGDP** | $5.5 \times 10^{-3}$ |

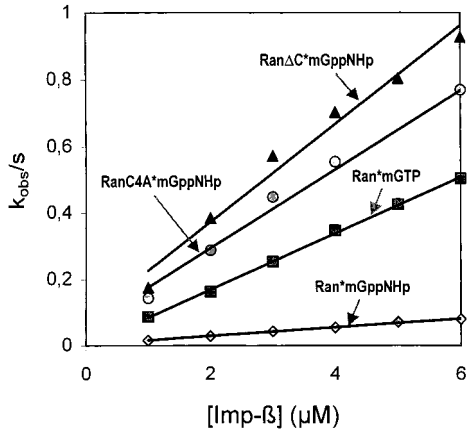


FIGURE 6: Effect of C-terminal modification in Ran on the dynamics of importin-$\beta$ binding. Different Ran constructs (200 nM) were mixed in an APP stopped-flow instrument with increasing concentrations of importin-$\beta$ (residues 1−462). Fluorescence traces were fitted as pseudo-first-order kinetics, and the resulting $k_{obs}$ values were plotted vs the concentration of importin-$\beta$: RanΔC·mGppNHp (▲), RanC4A·mGppNHp (●), Ran(fl)·mGTP (■), and Ran(fl)·mGppNHp (◆). In RanC4A, the natural C-terminal motif of residues $^{211}$DEDDDL$^{216}$ is replaced with $^{211}$AAAADL$^{216}$.

*Effect of the C-Terminal Domain of Ran on the Interaction with Importin-β.* It has been shown before that the C-terminal end of Ran is crucial for the interaction with RanBP1 (*33*) and that its loss reduces the binding affinity 10000-fold (*48*). For RanBD1, we find that the deletion of the C-terminal DEDDDL motif reduces the affinity for Ran·GppNHp 2000-fold (data not shown). This is in line with the crystal structure where the C-terminal end of Ran wraps around the RanBD1 such that the DEDDDL motif can dock onto a basic patch (*42*). Overlay assays with different GST constructs of the Ran protein revealed enhanced binding of importin-$\beta$ with the C-terminally truncated form GST-RanΔC, indicating an inhibitory effect of the DEDDDL sequence at the Ran C-terminus upon interaction of Ran with importin-$\beta$ (*63*).

To determine the effect of the Ran C-terminal end on the interaction with importin-$\beta$, we assessed the association of several Ran constructs with importin-$\beta$ and found an acceleration of the association reaction by a factor of 10 for the truncated RanΔC as compared to that of the wild-type Ran protein (Figure 6 and Table 3). The deletion of the C-terminal end increases the association rate such that importin-$\beta$ recognizes RanΔC even in the GDP-complexed state. Here importin-$\beta$ binds with a $K_D$ of ~5 $\mu$M with Ran·mGDP as determined by fluorescence kinetics. The inhibition effect of the acidic C-terminus in Ran upon binding of importin-$\beta$ is reduced if the negative charges are substituted by neutral side chains. A Ran mutant (RanC4A) in which four out of five aspartate and glutamate residues were substituted by alanine exhibits an increased association rate constant for association with importin-$\beta$ (R. Assheuer et al., manuscript in preparation).

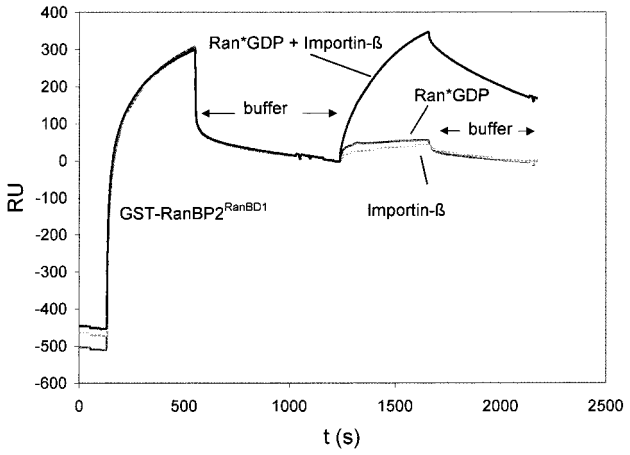


FIGURE 7: Formation of a complex formed by Ran·GDP, RanBD1, and importin-$\beta$. GST-RanBP2$^{RanBD1}$ was immobilized on the anti-GST matrix of a BIAcore sensor chip. Injection of either 1 $\mu$M Ran·GDP (dark gray) or importin-$\beta$ (residues 1−462, light gray) alone resulted in only a slight increase in the SPR signal. Only a mixture of Ran·GDP and importin-$\beta$ shows specific changes due to formation of the ternary complex (black trace).

A steric conflict between the Ran C-terminus and binding of importin-$\beta$ was illustrated by proteolytic digestion experiments. Carboxypeptidase A cleaves the 36 C-terminal amino acids of Ran·GppNHp in the complex with importin-$\beta$ as determined by mass spectroscopy (Figure 10), while no cleavage of Ran was observed for Ran·GppNHp complexed with RanBD1 or noncomplexed Ran·GDP.

*Ternary Complexes of Ran, RanBDi, and Importin-$\beta$.* Ran in its GTP-bound state is capable of binding a RanBD and an importin-$\beta$-like factor simultaneously (*31*, *45*, *64*−*67*), indicating separate bindings sites for both binding partners on Ran. This is supported by the three-dimensional structure of Ran·GppNHp complexed with RanBD1 (*42*) and importin-$\beta$ (*43*) or transportin (*44*). Ran·GDP exhibits only little [4 $\mu$M (*48*)] or no detectable affinity for RanBD*i* or importin-$\beta$ alone, but forms stable ternary complexes in the presence of both (N. C. Chi et al., 1996). While the first 200 amino acids of importin-$\beta$ have been reported to be sufficient for formation of the Ran·GTP·RanBD*i*·importin-$\beta$ complex, the corresponding GDP complex requires amino acids 1−352 of importin-$\beta$ (*64*).

These findings, together with the requirement of the C-terminal sequence of Ran for high-affinity binding of RanBP1, have prompted the model wherein RanBD*i* may unmask a region on Ran which is normally blocked by the C-terminus to allow binding of importin-$\beta$ (*63*). We investigated such a helper function of RanBD*i* for the binding of importin-$\beta$ to Ran by the BIAcore system. Importin-$\beta$ and Ran·GDP alone exhibit negligible, nonspecific binding toward GST·RanBD*i* on the sensor surface, while equimolar concentrations of Ran·GDP and importin-$\beta$ together result in significant binding (Figure 7). The dissociation of this ternary complex occurs much faster than the dissociation of binary complexes between Ran·GTP and RanBD*i* or importin-$\beta$ alone.

If binding of importin-$\beta$ to Ran·GTP is hindered by the Ran C-terminus (as shown in our stopped-flow experiments, Figure 6), complex formation with RanBP1 should accelerate the association reaction of Ran·GTP with importin-$\beta$. We verified such a contribution of RanBP1 upon the Ran·GTP·

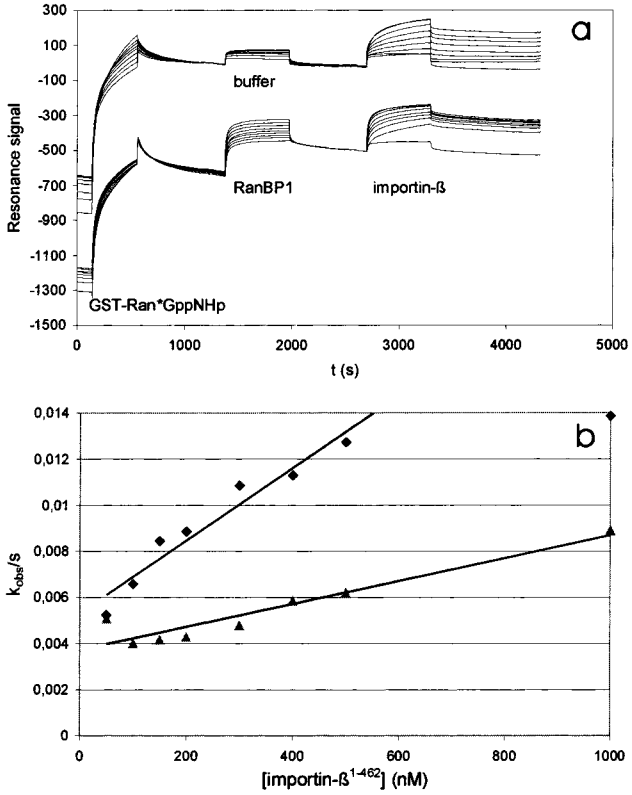


FIGURE 8: Effect of RanBP1 upon association of importin-$\beta$ with Ran·mGppNHp. (a) Sensogramms for the binding of importin-$\beta$ (residues 1−462) to GST-Ran·GppNHp in a BIAcore system after incubation of the Ran surface with either buffer or 500 nM RanBP1. Importin-$\beta$ concentrations were 0, 50, 100, 150, 200, 300, 400, and 500 nM. Curves were normalized according to the start of importin-$\beta$ injection (samples with RanBP1 treatment with an additional −500 RU shift for reasons of clarity). (b) Binding phases for importin-$\beta$ association with either GST·Ran·GppNHp (▲) or GST·Ran·GppNHp·RanBP1 complex (◆) were analyzed as monoexponential functions with the GraFit software. Apparent association rate constants are plotted vs the concentration of importin-$\beta$. Association rate constants at 20 °C for binding of importin-$\beta$ with GST·Ran·GppNHp·RanBP1 and GST·Ran·GppNHp are 1.6 $\times$ $10^4$ and 5.0 $\times 10^3$ $M^{-1}$ $s^{-1}$, respectively.

importin-$\beta$ dynamics in surface plasmon resonance (Figure 8a). Here, GST·Ran·GppNHp was captured by an anti-GST sera matrix and treated with either buffer or 500 nM RanBP1. After this, a series of various importin-$\beta$ concentrations was applied and the binding kinetics for importin-$\beta$ were analyzed as monoexponential functions. Indeed, importin-$\beta$ bound to GST·Ran·GppNHp·RanBP1 complexes about 3 times faster than to noncomplexed GST·Ran·GppNHp (Figure 8b).

*Costimulation of RanGAP-Catalyzed GTP Hydrolysis in Ran by Ran-Binding Domains.* RanBP1 was shown to enhance RanGAP-induced GTP hydrolysis in Ran by a factor of 10 (*34*). We tested if RanBD1 also enhances the GAP-stimulated GTPase reaction and whether the conserved RanBD domain itself is sufficient for the costimulation, or if the additional N- and C-terminal flanking amino acids in RanBP1 are necessary for this effect. Rna1p, the RanGAP homologue from *S. pombe*, which was shown to work efficiently on human Ran (*10*, *68*), was added to Ran complexed with [$\gamma$-$^{32}$P]GTP, and the production of radioactive $P_i$ was measured. RanGAP-stimulated GTP hydrolysis in Ran was enhanced by RanBD1 in the same manner as by RanBP1 (Figure 9a).

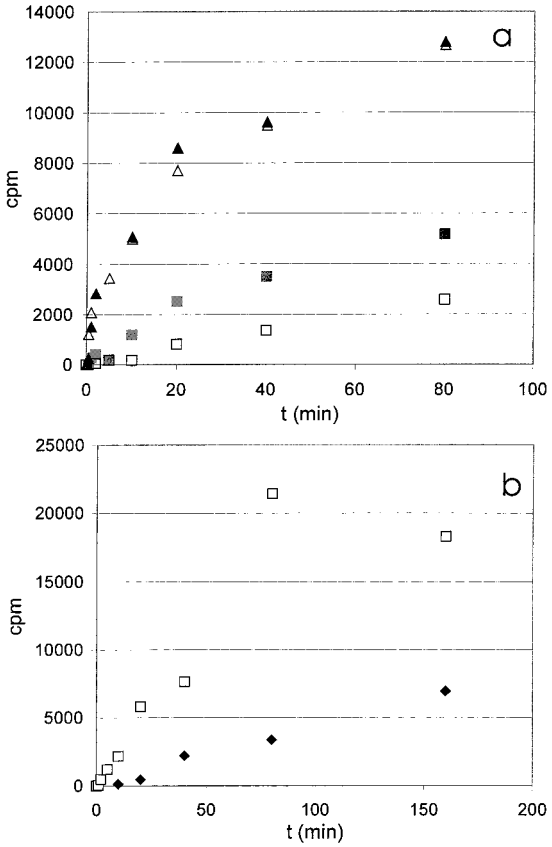


FIGURE 9: Effect of RanBD*i* on GTP hydrolysis in Ran A. Costimulation of Rna1-catalyzed GTP hydrolysis in Ran by GST-RanBP2$^{RanBD1}$. Ran (1 $\mu$M) preloaded with [$\gamma$-$^{32}$P]GTP was incubated with 150 pM Rna1p (*S. pombe*) in the presence of 2 $\mu$M RanBP1 or GST·RanBD1 at 30 °C. Aliquots of the reaction solution were mixed with charcoal at defined time points, and free $\gamma$-$^{32}$P was quantified in a scintillation counter: RanBP1 (△), GST-RanBD1 (▲), buffer (■), and the intrinsic rate (without Rna1p, □). (b) Overcoming the transportin blockade of Rna1-catalyzed GTP hydrolysis in Ran by GST-RanBP2$^{RanBD1}$. Ran (1 $\mu$M) preloaded with [$\gamma$-$^{32}$P]GTP was incubated with either 1 $\mu$M transportin alone (□) or 1 $\mu$M transportin and 2 $\mu$M GST-RanBD1 (◆) for 10 min, followed by addition of Rna1p (*S. pombe*) and incubation at 30 °C as described above. Data were corrected for background radioactivity.

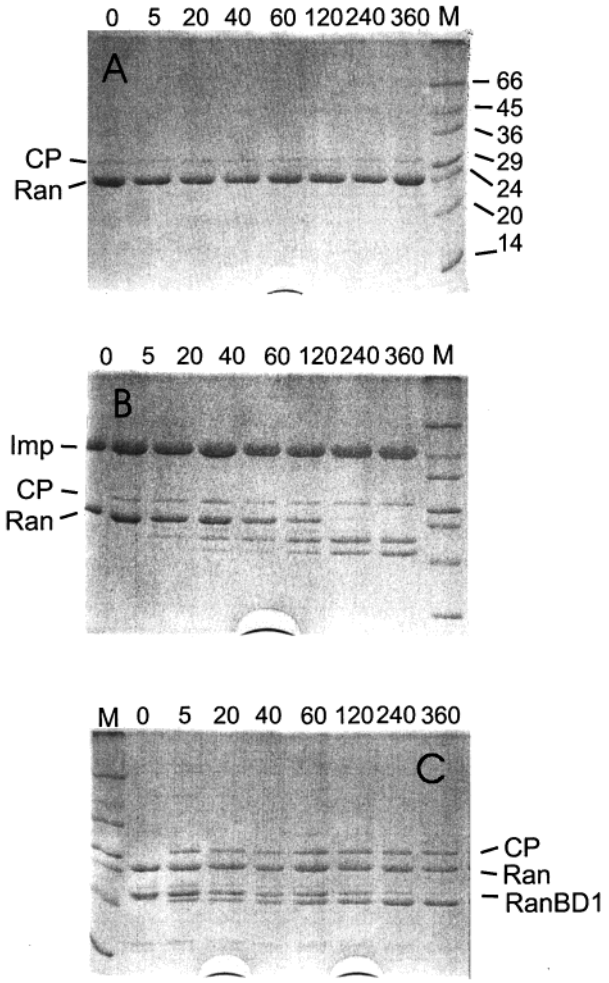


FIGURE 10: Proteolytic analysis of Ran complexes with carboxypeptidase A. Ran·GDP (A) and Ran·GppNHp complexed with either importin-$\beta$ (residues 1−462, B) or RanBD1 (C) were incubated with carboxypeptidase A for the indicated times. Aliquots of the protease digestion were analyzed by SDS−PAGE. While no proteolysis of the Ran band can be seen for Ran·GDP and the Ran·GppNHp·RanBD1 complex (there RanBD1 is degraded), there is a clear proteolytic digestion of Ran complexed with importin-$\beta$.

Importin-like proteins inhibit intrinsic and RanGAP-stimulated GTP hydrolysis in Ran (*28*, *65*). RanBP1 has been shown to overcome this blockade for importin-$\beta$ [in this case in concert with importin-α (*29*, *30*), RanBP7/importin 7 (*65*), transportin (*29*), importin 5/RanBP5 (*66*), CAS (*27*), exportin-t (*26*), and CRM1 (*69*, *70*)]. It was therefore interesting to know whether the RanBDs from RanBP2 can substitute for RanBP1 in this reaction. We therefore tested the effect of RanBD1 in a system with Ran·[$\gamma$-$^{32}$P]GTP, transportin, and Rna1p on GTP hydrolysis. Again, RanBD1 was sufficient to reconstitute the capability for GTP hydrolysis (Figure 9b).

## DISCUSSION

*Similar Affinities for Ran-Binding Domains from RanBP1 and RanBP2.* RanBP1 and RanBP2 share domains with high affinity for Ran·GTP. Quantifying the interaction of the four Ran-binding domains from RanBP2 with Ran·GppNHp yielded $K_D$ values between $10^{-9}$ and $10^{-8}$ M, with no significant differences between the individual domains and similar to the values measured for RanBP1. Microplate assays with purified RanBP2 and radiolabeled Ran·GTP resulted in an average affinity of Ran for RanBP2 of 0.5 nM (*58*). This value is identical with the lowest $K_D$ determined in our system at a similar ionic strength and 10-fold higher compared with the average affinity of all four RanBD*i*s. Taking into account the fact that the microplate assay includes several nonequilibria washing steps, one normally would expect an overestimation of the $K_D$ value or a value for the affinity lower than the real value. In our case, the discrepancies in affinity may be due to contributions of the GST moieties, additional stabilizing motifs of the RanBP2 protein which were absent from the expressed Ran-binding domains, or a cooperative effect of the RanBD*i* in the complete RanBP2.

Electron micrographs of nuclear pore complexes have localized RanBP2 to the fibrils (*57*) at the cytoplasmic side of the NPC. The lengths of purified RanBP2 after negative staining and that of the fibrils are very similar [36 and 35−50 nm, respectively (*71*)] and were seen as support for participation of RanBP2 in the formation of the fibril structures. The idea was proposed that a linear arrangement

of the four RanBD*i*s of RanBP2 on the fibrils could function as an affinity gradient for Ran·GTP, guiding the Ran transport complexes from low- to high-affinity binding sites along the cytoplasmic pore. Neither the similar affinities determined for the different RanBD*i*s for Ran·GTP nor the slow dissociation of Ran·GTP from the RanBD*i* can support such a model.

*Ran·GTP and Importin-$\beta$: Slowly but Tightly*. The association of Ran·GTP with importin-$\beta$ is slow but results in a highly stable complex. Affinities measured for Ran·mGTP and Ran·mGppNHp were on the order of 140 pM and 1 nM, respectively, and correspond to values (0.5 nM) determined indirectly for Ran·GTP and importin-$\beta$ in inhibition assays (*20*). We show that the dissociation of the binary complex occurs with half-times of days. This is at least 10 times slower than a first estimation for $k_{diss}$ based on filter binding assays with Ran·[$\gamma$-$^{32}$P]GTP and importin-$\beta$, where the rate of release of Ran from the complex was determined by Ran1-catalyzed GTP hydrolysis (*29*). We assume that the denaturation of Ran as seen in filter binding assays previously (*34*) has contributed to an overestimation of the amount of released radioactivity. With a $k_{diss}$ of $10^{-5}$ $s^{-1}$, spontaneous dissociation is much too slow for efficient nuclear transport.

Our experiments concerning the interaction between importin-$\beta$ and Ran in the triphosphate conformation have shown that care has to be taken concerning the utilization of nonhydrolyzable GTP analogues. Importin-$\beta$ clearly discriminates between Ran·mGTP and Ran·mGppNHp during the association reaction, whereas for RanBD*i*, the nature of the $\beta,\gamma$-bridging bond is not relevant. The structure of the Ran·GppNHp·importin-$\beta$ structure gives no obvious explanation for this behavior. Here, the $\beta,\gamma$-NH group is involved in a strong hydrogen bond with the main chain NH of Gly13 and a weak one with the side chain OH of Tyr39. However, all these interactions are far away from the Ran−importin interface and are unlikely to affect its structure. In structural studies on Ras, GTP- and GppNHp-bound complexes are found to be very similar (*72*). Refined investigations revealed that differences between Ras·GppNHp and Ras·GTP could be detected in catalytic loop 4 of the switch II region (*73*). Experiments with Ras and the catalytic domain of NF1 suggested that the dissociation rate constant for a Ras·mGppNHp·NF1 complex is about 10 times higher than for the corresponding Ras·mGTP complex (*74*).

The difference in binding affinity might be related to the dynamic behavior of Ran. P-NMR has shown two different chemical environments only for the $\gamma$-phosphate in Ran·GTP but not in Ran·GppNHp and that after saturation with RanBP1 only one of the two $\gamma$-phosphate environments remains in Ran·GTP (*75*).

*Antagonistic Role of the C-Terminal Region of Ran.* The acidic C-terminal sequence of the Ran protein is essential for fast binding to RanBD*i* (as shown here) as well as to RanBP1 (*48*). The opposite effect could be observed for importin-$\beta$. While formation of the complex between Ran and importin-$\beta$ is at least 1 order of magnitude slower than the same reaction with RanBD*i*, truncation of the acidic C-terminus of Ran causes a 10-fold increase in the association rate constant for importin-$\beta$. Analogous stronger binding of importin-$\beta$ to RanΔC·GTP (compared with Ran·GTP) under equilibrium conditions has been described previously in overlay assays (*45*).

Deleting the negative regulatory DEDDDL sequence allowed binding of importin-$\beta$ even to RanΔC in its GDP-bound state, resulting in a micromolar $K_D$ for the interaction between RanΔC·mGDP and importin-$\beta$. Further evidence for a direct competition between the Ran$^{DEDDDL}$ motif and importin-$\beta$ is derived from proteolytic digestion with carboxypeptidase A. Whereas the last 36 amino acids of Ran are cleaved in the complex with importin-$\beta$, they are not accessible in Ran·GDP alone or the Ran·GppNHpoRanBD1 complex.

Immunological experiments with antibodies directed against a peptide adjacent to the DEDDDL sequence showed recognition of Ran preferentially in the triphosphate state, indicating enhanced exposure of the C-terminus in Ran·GTP (*33*). A monoclonal antibody against the DEDDDL motif itself recognizes Ran only in the importin-$\beta$-complexed form of Ran·GTP and not in Ran·GTP alone (*76*). The structures of the Ran·GppNHp bound to a fragment of importin-$\beta$ (*43*) and to transportin (*44*) have shown that the C-terminal end is not necessary for the interaction and is actually either not visible in the structure (*43*) or only partially visible due to its involvement in crystal contacts (*44*). Although we do not have an easy explanation for the inhibitory role in the association reaction between Ran·GTP and importin, we assume that in the structure of Ran·GTP, which is not known at the present moment, the C-terminal end is located on Ran such that a contact site for importin binding is blocked and has to be rearranged before complex formation.

*Ran-Binding Domains: Enhancer or Terminator of the Ran−Effector Interaction?* In the structure of Ran·GppNHp complexed with RanBD1 of RanBP2 (*42*), the Ran C-terminus forms an almost complete turn that is wrapped around the surface of the RanBD1 moiety in what has been called a molecular embrace. This supports the idea that RanBP1 (or RanBD*i*) could open the importin-$\beta$ binding site on Ran by removing the steric hindrance of the acidic Ran C-terminus.

We could demonstrate by SPR experiments where we applied importin-$\beta$ to either immobilized GST·Ran·GppNHp alone or the preformed complex of RanBP1 that there is a clear enhancement of the association reaction by RanBD*i*. Therefore, it is assumed that RanBD*i* has a similar role as the deletion of the DEDDDL motif in removing the C-terminus from its original docking site at the Ran surface. This reorganization of the C-terminus may release a basic patch on the Ran surface which is composed of basic residues in helices $\alpha_3$ and $\alpha_4$ which we speculate to work as a positively charged docking site for the acidic DEDDDL sequence.

In our experiments, RanBD*i*s enhance binding of importin-$\beta$ with Ran·GTP and Ran·GDP. In the GTP-complexed state, they accelerate binding; in the case of Ran·GDP, binding of importin-$\beta$ with Ran can be detected only in the presence of RanBD*i*.

These results are somewhat in conflict with the finding that RanBD*i*s also have a clear role in mediating RanGAP-catalyzed GTP hydrolysis in Ran which is complexed with import or export receptors (*29*, *30*). Complete dissociation of an export complex formed by importin-$\alpha$, CAS, and Ran·GTP could be induced with RanBP1 (*29*). Our own results demonstrate that RanBD*i*s alone are sufficient to overcome the GTPase blockade by transportin; in the case of importin-

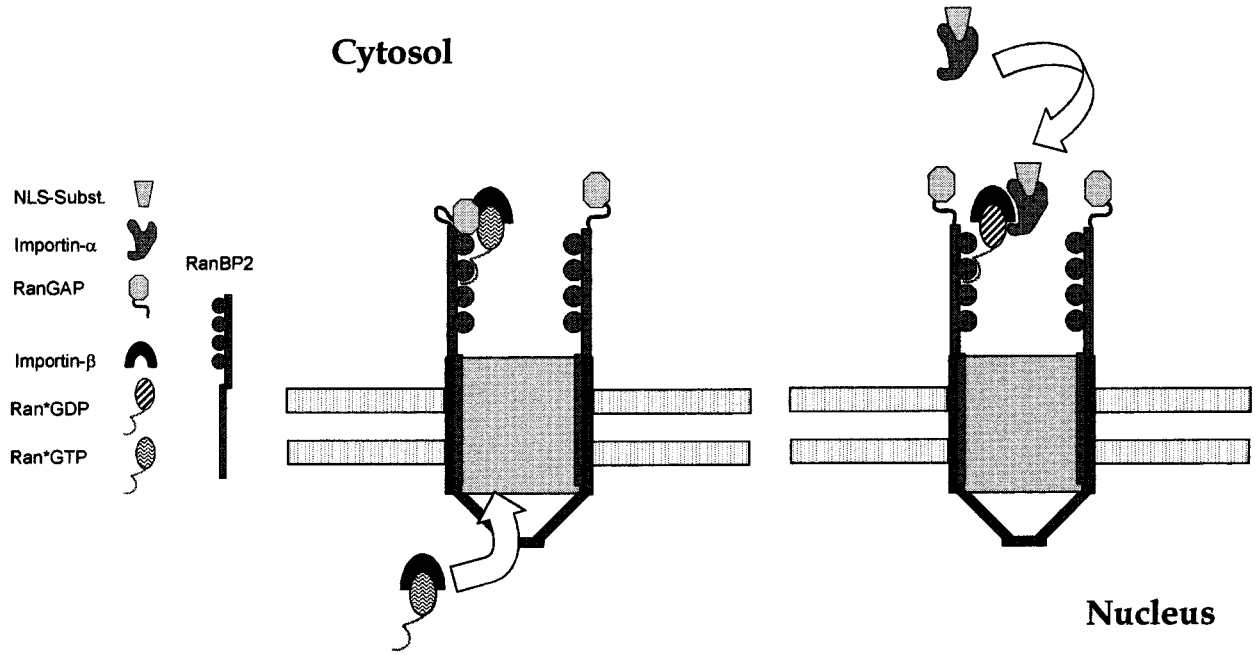


FIGURE 11: C-Terminus of Ran as a painter in nuclear export. Formation of the Ran·GTP·importin-$\beta$ complex terminates import of importin-$\beta$·importin-$\alpha$·NLS substrate trimers. Binding with importin-$\beta$ pushes the C-terminus of Ran into the solvent, where it is recognized by the RanBD*i* of RanBP2 when the complex leaves the nuclear pore. SUMO-modified RanGAP thereby has direct access for Ran·GTP and can stimulate GTP hydrolysis (left side). The residual affinity of the ternary complex between Ran·GDP, importin-$\beta$, and RanBD*i* is sufficiently high to retain importin-$\beta$ at the nuclear pore, increasing the efficiency in binding of the import substrate.

$\beta$, the release needs the presence of importin-$\alpha$ and RanBP1 (*29*, *30*). A partial competition between RanBD*i* and importin-$\beta$ for binding to Ran can be deduced from structural studies. In the Ran·GppNHp·RanBD1 structure, residues preceding $His^{17}$ of RanBD1 could not be traced in the electron density map. $His^{17}$ is located in the vicinity of the basic patch of Ran so that a substitution of $Ran^{DEDDL}$ by the acidic N-terminus of RanBD1 (DDDDDGP preceding $His^{17}$) is likely and may contribute to the high affinity of Ran for RanBD1. This idea is supported by the finding that N-terminally truncated RanBD1s lose the property to bind Ran·GTP completely (after trypsin cleavage, missing the first 31 N-terminal residues) or show a 50-fold drop in affinity (a RanBD1 construct starting at $His^{17}$, Zhao et al., unpublished data). In the Ran·importin-$\beta$ complex (*43*), the basic patch of Ran is deeply buried in the interface so that in the ternary complex importin-$\beta$ and RanBD*i* may compete for this contact point. The acidic N-terminus of the RanBD*i* can be modeled as a crowbar, fitting into a central cavity in the Ran·importin-$\beta$ complex. Obviously, this crowbar is not sufficient to dissociate the Ran·importin-$\beta$ complex without further support by importin-$\alpha$.

A better understanding of RanBD*i* in the release of complexes between Ran and import receptors should be achievable by dynamic and structural studies with transportin. This import receptor can be dissociated from Ran·GTP by RanBD*i* alone (without the need of additional factors) and therefore should show enhanced $k_{diss}$ rates in the presence of RanBD*i* (*29*).

Under physiological conditions, the acceleration of importin-$\beta$ binding with Ran by RanBD*i* may reflect a secondary effect. If the function of RanBP2 is to prevent escape of Ran·GTP (either alone or complexed with import or export receptors) into the cytosol, Ran has to bind RanBD*i* and importins or exportins simultaneously. If the Ran C-terminus is exposed to the solvent in complexes with importin-$\beta$, it may work like a tether. The RanBD*i* will catch the complex via the C-terminus of Ran, fix it at the nuclear pore in proximity to the SUMO-attached RanGAP, and support GTP hydrolysis in Ran. The residual binding affinity of the Ran·GDP·RanBD*i*·importin-$\beta$ complex should be sufficient to keep importin-$\beta$ at the NPC, leading to a more efficient initiation of the next import cycle by binding of the new import substrate (Figure 11). Further insight into the role of RanBD*i* in the formation and disassembly of import and export complexes should be achieved by determining the structure of ternary complexes between Ran, RanBD*i*, and importin-$\beta$ or transportin, the binary complex of RanBD*i* and Ran·GDP, and Ran·GTP without further binding partners.

## ACKNOWLEDGMENT

We thank Drs. Jörg Becker and Ingrid Vetter for discussion, Roman Hillig for providing us with samples of rna1 (*S. pombe*), and Heino Prinz for MS analysis of protein samples.

## REFERENCES

1. Stoffler, D., Fahrenkrog, B., and Aebi, U. (1999) *Curr. Opin. Cell Biol. 11*, 391−401.
2. Bischoff, F. R., and Ponstingl, H. (1991) *Nature 354*, 80−82.
3. Drivas, G. T., Shih, A., Coutavas, E., Rush, M. G., and Deustachio, P. (1990) *Mol. Cell. Biol. 10*, 1793−1798.
4. Melchior, F., Weber, K., and Gerke, V. (1993) *Mol. Biol. Cell 4*, 569−581.
5. Moore, M. S., and Blobel, G. (1993) *Nature 365*, 661−663.
6. Bischoff, F. R., and Ponstingl, H. (1991) *Nature 354*, 80−82.
7. Klebe, C., Bischoff, F. R., Ponstingl, H., and Wittinghofer, A. (1995) *Biochemistry 34*, 639−647.
8. Klebe, C., Prinz, H., Wittinghofer, A., and Goody, R. S. (1995) *Biochemistry 34*, 12543−12552.

9. Ohtsubo, M., Okazaki, H., and Nishimoto, T. (1989) *J. Cell Biol. 109*, 1389−1397.
10. Becker, J., Melchior, F., Gerke, V., Bischoff, F. R., Ponstingl, H., and Wittinghofer, A. (1995) *J. Biol. Chem. 270*, 11860−11865.
11. Bischoff, F. R., Klebe, C., Kretschmer, J., Wittinghofer, A., and Ponstingl, H. (1994) *Proc. Natl. Acad. Sci. U.S.A. 91*, 2587−2591.
12. Bischoff, F. R., Krebber, H., Kempf, T., Hermes, I., and Ponstingl, H. (1995) *Proc. Natl. Acad. Sci. U.S.A. 92*, 1749−1753.
13. Mahajan, R., Gerace, L., and Melchior, F. (1998) *J. Cell Biol. 140*, 259−270.
14. Matunis, M. J., Wu, J., and Blobel, G. (1998) *J. Cell Biol. 140*, 499−509.
15. Saitoh, H., Cooke, C. A., Burgess, W. H., Earnshaw, W. C., and Dasso, M. (1996) *Mol. Biol. Cell 7*, 1319−1334.
16. Görlich, D., and Kutay, U. (1999) *Annu. Rev. Cell Dev. Biol. 15*, 607−660.
17. Pemberton, L. F., Blobel, G., and Rosenblum, J. S. (1998) *Curr. Opin. Cell Biol. 10*, 392−399.
18. Hood, J. K., and Silver, P. A. (1999) *Curr. Opin. Cell Biol. 11*, 241−247.
19. Dahlberg, J. E., and Lund, E. (1998) *Curr. Opin. Cell Biol. 10*, 400−408.
20. Görlich, D., Pante, N., Kutay, U., Aebi, U., and Bischoff, F. R. (1996) *EMBO J. 15*, 5584−5594.
21. Izaurralde, E., Kutay, U., Von Kobbe, C., Mattaj, I. W., and Görlich, D. (1997) *EMBO J. 16*, 6535−6547.
22. Rexach, M., and Blobel, G. (1994) *Cell 83*, 683−692.
23. Siomi, M. C., Eder, P. S., Kataoka, N., Wan, L., Liu, Q., and Dreyfuss, G. (1997) *J. Cell Biol. 138*, 1181−1192.
24. Arts, G. J., Fornerod, M., and Mattaj, I. W. (1998) *Curr. Biol. 8*, 305−314.
25. Fornerod, M., Ohno, M., Yoshida, M., and Mattaj, I. W. (1997) *Cell 90*, 1051−1060.
26. Kutay, U., Lipowsky, G., Izaurralde, E., Bischoff, F., Schwarzmaier, P., Hartmann, E., and Görlich, D. (1998) *Mol. Cell 1*, 359−369.
27. Kutay, U., Bischoff, F. R., Kostka, S., Kraft, R., and Görlich, D. (1997) *Cell 90*, 1061−1071.
28. Floer, M., and Blobel, G. (1996) *J. Biol. Chem. 271*, 5313−5316.
29. Bischoff, F. R., and Görlich, D. (1997) *FEBS Lett. 419*, 249−254.
30. Floer, M., Blobel, G., and Rexach, M. (1997) *J. Biol. Chem. 272*, 19538−19546.
31. Lounsbury, K. M., and Macara, I. G. (1997) *J. Biol. Chem. 272*, 551−555.
32. Coutavas, E., Ren, M., Oppenheim, J. D., D'Eustachio, P., and Rush, M. G. (1993) *Nature 366*, 585−587.
33. Richards, S. A., Lounsbury, K. M., and Macara, I. G. (1995) *J. Biol. Chem. 270*, 14405−14411.
34. Bischoff, F. R., Krebber, H., Smirnova, E., Dong, W., and Ponstingl, H. (1995) *EMBO J. 14*, 705−715.
35. Richards, S. A., Lounsbury, K. M., Carey, K. L., and Macara, I. G. (1996) *J. Cell Biol. 134*, 1157−1168.
36. Schlenstedt, G., Wong, D. H., Koepp, D. M., and Silver, P. A. (1995) *EMBO J. 14*, 5367−5378.
37. Dingwall, C., Kandelslewis, S., and Seraphin, B. (1995) *Proc. Natl. Acad. Sci. U.S.A. 92*, 7525−7529.
38. Hartmann, E., and Görlich, D. (1995) *Trends Cell Biol. 5*, 192−193.
39. Wu, J., Matunis, M. J., Kraemer, D., and Coutavas, E. (1995) *J. Biol. Chem. 270*, 14209−14213.
40. Yokoyama, N., Hayashi, N., Seki, T., Panté, N., Ohba, T., Nishii, K., Kuma, K., Hayashida, T., Miyata, T., Aebi, U., Fukui, M., and Nishimoto, T. (1995) *Nature 376*, 184−188.
41. Matunis, M. J., Coutavas, E., and Blobel, G. (1996) *J. Cell Biol. 135*, 1457−1470.
42. Vetter, I. R., Nowak, C., Nishimoto, T., Kuhlmann, J., and Wittinghofer, A. (1999) *Nature 398*, 39−46.
43. Vetter, I. R., Arndt, A., Kutay, U., Görlich, D., and Wittinghofer, A. (1999) *Cell 97*, 635−646.
44. Chook, Y. M., and Blobel, G. (1999) *Nature 399*, 230−237.
45. Lounsbury, K. M., Richards, S. A., Perlungher, R. R., and Macara, I. G. (1996) *J. Biol. Chem. 271*, 2357−2360.
46. Yaseen, N. R., and Blobel, G. (1999) *J. Biol. Chem. 274*, 26493−26502.
47. Klebe, C., Nishimoto, T., and Wittinghofer, F. (1993) *Biochemistry 32*, 11923−11928.
48. Kuhlmann, J., Macara, I., and Wittinghofer, A. (1997) *Biochemistry 36*, 12027−12035.
49. Kutay, U., Izaurralde, E., Bischoff, F. R., Mattaj, I. W., and Görlich, D. (1997) *EMBO J. 16*, 1153−1163.
50. Hiratsuka, T. (1983) *Biochim. Biophys. Acta 742*, 496−508.
51. John, J., Sohmen, R., Feuerstein, J., Linke, R., Wittinghofer, A., and Goody, R. S. (1990) *Biochemistry 29*, 6058−6065.
52. Bradford, M. M. (1976) *Anal. Biochem. 72*, 248−254.
53. Lenzen, C., Cool, R. H., Prinz, H., Kuhlmann, J., and Wittinghofer, A. (1998) *Biochemistry 37*, 7420−7430.
54. Beddow, A. L., Richards, S. A., Orem, N. R., and Macara, I. G. (1995) *Proc. Natl. Acad. Sci. U.S.A. 92*, 3328−3332.
55. Blomberg, N., Baraldi, E., and Nilges, M. (1999) *Trends Biochem. 24*, 441−445.
56. Carl, U. D., Pollmann, M., Orr, E., Gertler, F. B., Chakraborty, T., and Wehland, J. (1999) *Curr. Biol. 9*, 715−718.
57. Pante, N., and Aebi, U. (1996) *Curr. Opin. Cell Biol. 8*, 397−406.
58. Delphin, C., Guan, T., Melchior, F., and Gerace, L. (1997) *Mol. Biol. Cell 8*, 2379−2390.
59. Koepp, D. M., and Silver, P. A. (1996) *Cell 87*, 1−4.
60. Chaiken, I., Rose, S., and Karlsson, R. (1992) *Anal. Biochem. 201*, 197−210.
61. VanCott, T. C., Loomis, L. D., Redfield, R. R., and Birx, D. L. (1992) *J. Immunol. Methods 146*, 163−176.
62. Malmborg, A. C., Michaelsson, A., Ohlin, M., Jansson, B., and Borrebaeck, C. A. (1992) *Scand. J. Immunol. 35*, 643−650.
63. Lounsbury, K. M., Richards, S. A., Carey, K. L., and Macara, I. G. (1996) *J. Biol. Chem. 271*, 32834−32841.
64. Chi, N. C., Adam, E. J. H., and Adam, S. A. (1997) *J. Biol. Chem. 272*, 6818−6822.
65. Görlich, D., Dabrowski, M., Bischoff, F., Kutay, U., Bork, P., Hartmann, E., and Izaurralde, E. (1997) *J. Cell Biol. 138*, 65−80.
66. Deane, R., Schafer, W., Zimmermann, H. P., Mueller, L., Görlich, D., Prehn, S., Ponstingl, H., and Bischoff, F. R. (1997) *Mol. Cell. Biol. 17*, 5087−5096.
67. Schlenstedt, G., Smirnova, E., Deane, R., Solsbacher, J., Kutay, U., Gorlich, D., Ponstingl, H., and Bischoff, F. R. (1997) *EMBO J. 16*, 6237−6249.
68. Hillig, R. C., Renault, L., Vetter, I. R., Drell, T., and Becker, J. (1999) *Mol. Cell 3*, 781−791.
69. Paraskeva, E., Izaurralde, E., Bischoff, F. R., Huber, J., Kutay, U., Hartmann, E., Luhrmann, R., and Görlich, D. (1999) *J. Cell Biol. 145*, 255−264.
70. Kehlenbach, R. H., Dickmanns, A., Kehlenbach, A., Guan, T. L., and Gerace, L. (1999) *J. Cell Biol. 145*, 645−657.
71. Jarnik, M., and Aebi, U. (1998) *J. Struct. Biol. 107* (3), 291−308.
72. Schlichting, I., Almo, S. C., Rapp, G., Wilson, K., Petratos, K., Lentfer, A., Wittinghofer, A., Kabsch, W., Pai, E. F., Petsko, G. A., et al. (1990) *Nature 345*, 309−315.
73. Scheidig, A. J., Burmester, C., and Goody, R. S. (1999) *Structure 7*, 1311−1324.
74. Ahmadian, M. R., Hoffmann, U., Goody, R. S., and Wittinghofer, A. (1997) *Biochemistry 36*, 4535−4541.
75. Geyer, M., Assheuer, R., Klebe, C., Kuhlmann, J., Becker, J., Wittinghofer, A., and Kalbitzer, H. R. (1999) *Biochemistry 38*, 11250−11260.
76. Hieda, M., Tachibana, T., Yokoya, F., Kose, S., Imamoto, N., and Yoneda, Y. (1999) *J. Cell Biol. 144*, 645−655.


BI001010F